crystals

MDPI

Communication

4-Phenylnaphtho[2,3-*c*]furan-1(3*H*)-one, 9-Phenylnaphtho[2,3-*c*]furan-1(3*H*)-one and 3*a*,4-Dihydro-9-phenylnaphtho[2,3-*c*]furan-1(3*H*)-one Crystal Structures

Nabyl Merbouh, Simon Cassegrain and Wen Zhou *

Department of Chemistry, Simon Fraser University, 8888 University Drive, Burnaby, BC V5A 1S6, Canada; nmerbouh@sfu.ca (N.M.); simon_cassegrain@sfu.ca (S.C.)
* Correspondence: wza54@sfu.ca

Abstract: The crystal structures are reported for two unsubstituted arylnaphthalene lactones, 4-phenylnaphtho[2,3-*c*]furan-1(3*H*)-one (2), 9-phenylnaphtho[2,3-*c*]furan-1(3*H*)-one (3) and a non-aromatic dihydro arylnaphthene lactone, 3*a*,4-dihydro-9-phenylnaphtho[2,3-*c*]furan-1(3*H*)-one (5). There are only minor differences in the geometrical parameters of these structures. However, in certain cases, both isomers of arylnaphthalene lactones (termed Type I and Type II) were found in the same asymmetric unit cell.

Keywords: crystal structure; arylnaphthalene lactones; position isomers; mixture of isomers

Citation: Merbouh, N.; Cassegrain, S.; Zhou, W. 4-Phenylnaphtho[2,3-*c*]furan-1(3*H*)-one, 9-Phenylnaphtho [2,3-*c*]furan-1(3*H*)-one and 3*a*,4-Dihydro-9-phenylnaphtho[2,3-*c*]furan-1(3*H*)-one Crystal Structures. *Crystals* **2021**, *11*, 857. https://doi.org/10.3390/cryst11080857

Academic Editor: Vladislav V. Gurzhiy

Received: 6 July 2021
Accepted: 19 July 2021
Published: 23 July 2021

1. Introduction

Arylnaphtalene lactones are a subclass of lignans that can be extracted from a wide range of species such as *Justicia* [1]. These derivatives, due to their wide variety of biological activities such as antifungal [2], antileishmanial [2], antiviral [3,4] and anti-inflammatory [5] are now widely studied as potential therapeutic leads. Several arylnaphtalene lactones have been extracted from a variety of plants and are divided into two types (Type I and Type II) corresponding to the position of the lactone on the molecular system [6,7]. Furthermore, for the past two decades, many pathways for the synthesis of these molecules and their numerous scaffolds' assembly have been investigated in order to further study their bioactivities [8–15].

Of the many synthetic routes explored to efficiently obtain these arylnapthalene lactones, intramolecular Diels–Alder methods [8], multicomponent methods [9], Suzuki cross-coupling reactions [10], oxidative cyclizations [11], silver-catalyzed one-pot synthesis [12] and metal-catalyzed annulations [13–15] are just a sample of the possible synthetic pathways available. Each of these approaches allow access to a large variety of original lactones, bearing a variety of substituents along the conjugated backbone.

For many arylnapthalene lactones, isolated or synthesized, several crystal structures have been published. However, to our knowledge, no crystal structures of their bare scaffolds have been investigated. Such a structural investigation is an essential element for a better understanding of the structure–property relationship and the bioactivities associated with these lignans. Furthermore, these crystal structures could provide the insight necessary to implement further modification to their conjugated backbones without interfering with their overall structural scaffolds.

In this communication, we focused on the heat-mediated Dehydro-Diels–Alder synthetic approach to these arylnaphthalene lactones [16–18]. This approach not only yielded both arylnaphthalene lactone types (Type I and II) in good yields and purity, but interestingly showed a dramatic solvent effect. Indeed, when the solvent was switched from toluene to ethanol, a partially aromatic arylnaphthalene lactone was the main product of

the reaction (Scheme 1). Additionally, both Type I and Type II were found to co-crystallize in the same asymmetric cell unit: an interesting crystal structure with two different isomers with different properties such as melting point and polarity.

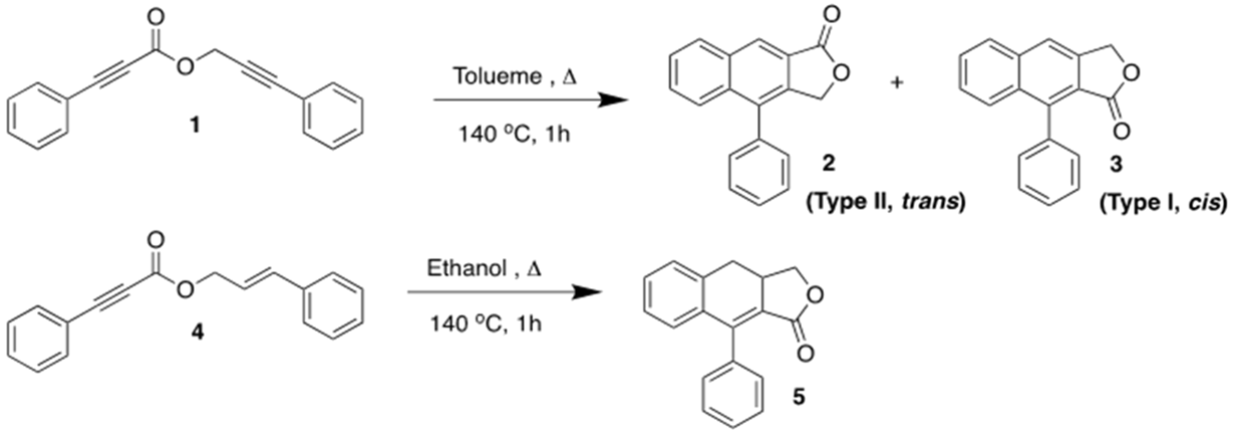

Scheme 1. Synthesis of lactones 2, 3 and 5.

2. Materials and Instrumentation

All reagents and solvents were purchased from Sigma-Aldrich and used without further purification. All NMR spectra were recorded on a Bruker Avance III 400 MHz or a Bruker Avance III 500 MHz spectrometer and were referenced to the residual chloroform ($CDCl_3$) resonance at 7.26 ppm for proton and 77.16 ppm for carbon. All cyclization reactions were performed on a 6 mL scale using toluene or ethanol as a solvent in an Anton Parr Monowave 50 reactor at 140 °C in a 10 mL capped vial fitted with a magnetic stir bar. All chromatography separations were performed on a Teledyne Combiflash system using silica gel disposable flash columns (Redi*Sep* Rf, normal phase, 40–60 micron) and ethyl acetate/hexanes mixtures as eluent. All TLC analyses were performed on aluminum backed plates pre-coated with silica gel (Merck, Silica Gel 60 F254) and visualized by UV light.

2.1. Synthesis

2.1.1. Synthesis of 3-Phenylprop-2-yn-1-yl 3-phenylpropiolate (**1**) and Trans-cinnamyl 3-phenylpropiolate (**4**)

General method: tthe acid (2.05 mmol, 1 equiv.) and 4-dimethylaminopyridine (0.15 mmol, 0.07 equiv.), solution of cinnamyl alcohol (1.85 mmol, 0.9 equiv.) in dichloromethane (DCM, 10 mL) and *N*-(3-Dimethylaminopropyl)-*N*′-ethylcarbodiimide hydrochloride (EDCI, 2.46 mmol, 1.2 equiv.) were added to a flame-dried 5 mL two-necked round-bottom flask that was equipped with an argon inlet adapter, a septum and a stir bar. The reaction mixture was stirred at room temperature for 3 h and diluted with DCM (15 mL) followed by filtration through a plug of silica gel. The crude material was subsequently concentrated under reduced pressure to yield the desired ester. When the NMR showed traces of either the starting material or a coupling agent, the crude was simply dissolved in DCM (10 mL) and filtered one more time through another silica gel plug. This second filtration yielded high grade material suitable for subsequent steps without further purification.

3-Phenylprop-2-yn-1-yl 3-phenylpropiolate (**1**) Isolated as a yellow solid in 80% yield, mp: 48–52 °C. Spectral data are in accordance with the literature [17]. ^{1}H NMR (400 MHz, $CDCl_3$) δ 7.63–7.57 (m, 2H), 7.50–7.43 (m, 3H), 7.42–7.27 (m, 5H), 5.07 (s, 2H) ppm (see Figure S1). ^{13}C NMR (101 MHz, $CDCl_3$) δ 153.4, 133.4, 132.1, 131.0, 129.1, 128.8, 128.5, 122.1, 119.6, 87.6, 87.5, 82.1, 80.2, 54.3 ppm (see Figure S1).

trans-Cinnamyl 3-phenylpropiolate (**4**) Isolated as a clear oil in 72% yield. Spectral data are in accordance with the literature [16]. ^{1}H NMR (400 MHz, $CDCl_3$) δ 7.66–7.59 (m, 2H),

7.51–7.27 (m, 8H), 6.76 (d, *J* = 15.9 Hz, 1H), 6.37 (dt, *J* = 15.9, 6.6 Hz, 1H), 4.92 (dd, *J* = 6.6, 1.2 Hz, 2H) ppm (see Figure S2). ^{13}C NMR (101 MHz, $CDCl_3$) δ 154.0, 136.1, 135.5, 133.1, 130.8, 128.8, 128.7, 128.4, 126.8, 122.2, 119.7 86.8, 80.6, 66.7.ppm (see Figure S2).

2.1.2. Synthesis of 4-Phenylnaphtho [2,3-c]furan-1(3H)-one (**2**) and 9-Phenylnaphtho [2,3-c]furan-1(3H)-one (**3**)

3-Phenylprop-2-yn-1-yl 3-phenylpropiolate **1** (150 mg) was dissolved in toluene (6 mL) and the solution was irradiated in an Anton Parr Monowave 50 reactor at 140 °C for one hour with constant stirring. After irradiation, the ethanol was removed under vacuum and the reaction mixture was purified using a Teledyne Combiflash system that used ethyl acetate/hexanes mixture as an eluent to yield two fractions containing compounds lactone **2** (TLC R*f* = 0.40 (15% ethyl acetate/hexanes) and lactone **3** TLC R*f* = 0.20 (15% ethyl acetate/hexanes). After the evaporation of the solvent, both lactones were recrystallized from a mixture of 15% ethyl acetate/hexanes.

4-Phenylnaphtho[2,3-c]furan-1(3H)-one (**2**) [17]. Isolated as a white solid, mp 158–160 °C. ^{1}H NMR (400 MHz, $CDCl_3$) δ 8.52 (s, 1H), 8.09 (d, 1H, *J* = 7.03 Hz), 7.81 (d, 1H, *J* = 7.03 Hz), 7.62–7.51 (m, 5H), 7.39 (d, 2H, *J* = 6.64 Hz), 5.27 (s, 2H) ppm (see Figure S3). ^{13}C NMR (101 MHz, $CDCl_3$) δ 171.3, 138.6, 136.0, 135.0, 134.3, 133.9, 130.3, 129.5, 129.2, 129.2, 128.6, 126.9, 126.6, 126.1, 123.2, 69.7 ppm (see Figure S3).

9-Phenylnaphtho[2,3-c]furan-1(3H)-one (**3**) [17]. Isolated as a white solid, mp 174–176 °C. ^{1}H NMR (400 MHz, $CDCl_3$) δ 7.96 (d, 1H, *J* = 8.30 Hz), 7.90 (s, 1H), 7.81 (d, 1H, *J* = 8.79 Hz), 7.64 (t, 1H, *J* = 7.32 Hz), 7.54–7.52 (m, 2H), 7.48 (t, 1H, *J* = 7.32 Hz), 7.39–7.37 (m, 2H), 5.45 (s, 2H) ppm (see Figure S4). ^{13}C NMR (101 MHz, $CDCl_3$) δ 169.7, 142.4, 140.3, 136.4, 134.6, 133.0, 130.2, 128.8, 128.4, 128.3, 128.2, 128.2, 126.9, 120.4, 120.1, 68.3 ppm (see Figure S4).

2.1.3. Synthesis of 3*a*,4-Dihydro-9-phenylnaphtho[2,3-*c*]furan-1(3*H*)-one (**5**)

trans-Cinnamyl 3-phenylpropiolate **4** (150 mg) was dissolved in ethanol (6 mL) and the solution was irradiated in an Anton Parr Monowave 50 reactor at 140 °C for one hour with constant stirring. After irradiation, the ethanol solution was cooled to room temperature, during which time lactone **5** started crystalizing as needles that were isolated by filtration [12].

*3a,4-Dihydro-9-phenylnaphtho[2,3-c]furan-1(3H)-one. (**5**)* Isolated as a white solid, mp: 183–186 °C. ^{1}H NMR (400 MHz, CD_2Cl_2) δ 7.46–7.43 (m, 3H), 7.33–7.26 (m, 4H), 7.19–7.15 (m, 1H), 6.91 (d, *J* = 7.8 Hz, 1H), 4.72 (t, *J* = 8.8 Hz, 1H), 4.04 (t, *J* = 8.8 Hz, 1H), 3.50–3.40 (m, 1H), 3.07 (dd, *J* = 6.6, 15.0 Hz, 1H), 2.88 (t, *J* = 15.4 Hz, 1H) ppm (see Figure S5). ^{13}C NMR (101 MHz, CD_2Cl_2) δ 168.6, 147.2, 136.3, 136.1, 135.2, 130.2, 128.7, 128.5, 128.2, 127.5, 122.9, 71.7, 36.0, 33.2. ppm (see Figure S5).

2.2. X-ray Analysis

X-ray Crystallography: suitable crystals were coated in paratone oil and mounted on a MiTeGen Micro Mount. All the relevant data were collected on a Bruker Smart instrument equipped with a Photon II CCD area detector fixed at a distance of 5.0 cm from the crystal and a Mo Kα fine focus sealed tube (λ = 0.71073 nm) operated at 1.5 kW (50 kV, 30 mA), filtered with a graphite monochromator.

Data were collected and integrated using the Bruker SAINT software package [18] and were corrected for absorption effects using the multi-scan technique (SADABS) [19] or (TWINABS) [20,21]. All structures were solved by direct methods [22,23]. All non-hydrogen atoms were refined anisotropically. All hydrogen atoms were placed in calculated positions with isotropic refines and U values 1.2 times greater than the U(eq) value of the corresponding non-hydrogen atom. All refinements were performed using the SHELXTL crystallographic software package of Bruker-AXS [24]. The molecular drawings were generated by the use of POV-RAY [25]. The **mixture 2**,**3** crystallized with two isomers in the asymmetric unit and was modeled in two orientations (44 and 56%). Additional crystallographic information can be found in Table 1.

Table 1. Crystallographic data and structure refinement details for **2**, **3**, **mixture 2–3** and **5**.

Identification Code	**2**	**3**	**Mixture 2–3**	**5**
Empirical formula	$C_{18}H_{12}O_2$	$C_{18}H_{12}O_2$	$C_{18}H_{14}O_2$	$C_{18}H_{14}O_2$
Formula weight	260.28	260.28	262.29	262.29
Temperature/K	296(2)	296(2)	296(2)	296(2)
Crystal system	monoclinic	monoclinic	monoclinic	monoclinic
Space group	$P2_1/c$	$P2_1/c$	$P2_1/c$	$P2_1/n$
a/Å	10.0988(5)	9.1899(10)	9.2069(17)	6.0820(2)
b/Å	16.7625(8)	17.7239(16)	17.797(3)	18.7457(8)
c/Å	8.0793(4)	7.7263(8)	7.7530(17)	11.6861(5)
α/°	90	90	90	90
β/°	94.699(2)	91.711(4)	91.170(8)	98.759(2)
γ/°	90	90	90	90
Volume/Å^3	1363.08(12)	1257.9(2)	1270.1(4)	1316.81(9)
Z	4	4	4	4
ρ_{calc}g/cm^3	1.268	1.374	1.372	1.323
μ/mm^{-1}	0.082	0.089	0.088	0.085
Radiation	MoKα (λ = 0.71073)	MoKα (λ = 0.71073)	MoKα (λ = 0.71073)	MoKα (λ = 0.71073)
2Θ range for data collection/°	4.72 to 60.094	4.434 to 58.288	4.424 to 58.366	4.142 to 61.038
Index ranges	$-14 \leq h \leq 14$, $-23 \leq k \leq 23$, $-11 \leq l \leq 11$	$-12 \leq h \leq 12$, $-24 \leq k \leq 22$, $-8 \leq l \leq 10$	$-12 \leq h \leq 12$, $-24 \leq k \leq 24$, $-10 \leq l \leq 10$	$-8 \leq h \leq 7$, $-26 \leq k \leq 26$, $-16 \leq l \leq 16$
Reflections collected	32,430	15,890	22,604	28,192
Independent reflections	3988 [R_{int} = 0.0239, R_{sigma} = 0.0151]	3393 [R_{int} = 0.0534, R_{sigma} = 0.0414]	3436 [R_{int} = 0.0467, R_{sigma} = 0.0308]	4018 [R_{int} = 0.0337, R_{sigma} = 0.0232]
Data/restraints/parameters	3988/0/181	3393/0/181	3436/2/207	4018/0/181
Goodness-of-fit on F^2	1.105	1.075	1.047	1.137
Final R indexes [I > = 2σ (I)]	R_1 = 0.0842, wR_2 = 0.2262	R_1 = 0.0458, wR_2 = 0.1242	R_1 = 0.0495, wR_2 = 0.1388	R_1 = 0.0634, wR_2 = 0.1530
Final R indexes [all data]	R_1 = 0.1191, wR_2 = 0.2543	R_1 = 0.0739, wR_2 = 0.1470	R_1 = 0.0653, wR_2 = 0.1484	R_1 = 0.0896, wR_2 = 0.1769
Largest diff. peak/hole/e Å^{-3}	1.04/−1.04	0.49/−0.34	0.25/−0.18	0.96/−1.02

3. Results

The crystal structures of **2**, **3**, **mixture 2–3** and **5** were determined by single-crystal X-ray diffraction and are shown in Figure 1 along with the atomic numbering schemes. In the **mixture 2–3**, both *cis* and *trans* isomers of arylnaphthalene lactones (Type I and Type II, respectively) were found in the same asymmetric unit cell, and they were molded in two orientations as *cis* isomers (O3 57.7%) and *trans* isomers (O2 42.3%). These unique co-crystallized isomers are stabilized by hydrogen bond interactions between O3-H14, O3-H16 and O2-H1, O2-H2 (shown in Figure S6). For all structures, the torsion angles (°) between the phenyl group and the naphthoquinone moiety are shown in Figure 2 and were found to be 62.43 and 62.85° in structure **3** and the **mixture 2–3**, respectively. On the other hand, the large torsion angle of 68.12° in structure **2** may have been due to less steric hindrance of the *trans* ketone group. For compound **5**, an intermediate species in the reaction, however, the presence of an sp^3 hybridized carbon C8 in the lactone did not allow

for the measurement of the torsion angle due to the non-planarity and non-aromaticity of the structure.

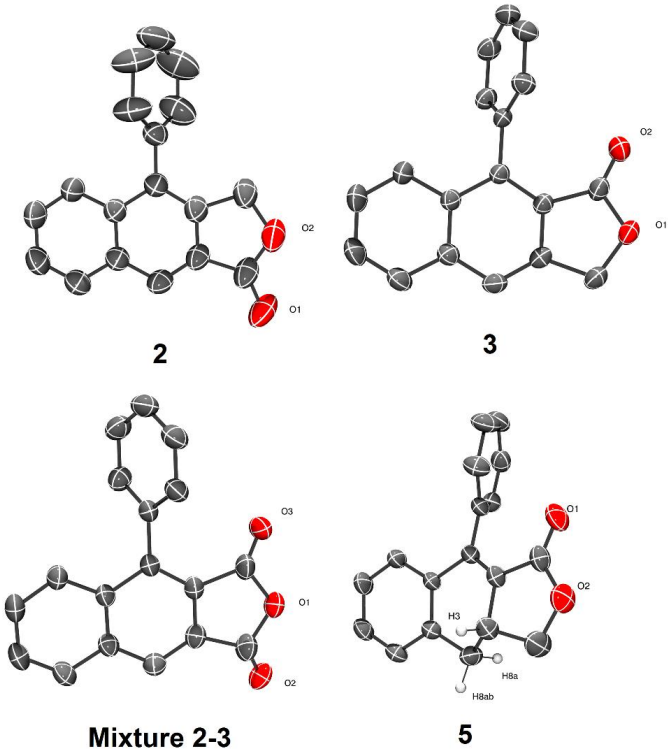

Figure 1. Molecular structures (50% ellipsoids) of **2**, **3**, **mixture 2–3** and **5**. All H atoms are omitted for clarity except for **5**, which can be found and refined. Selected bond lengths [Å]: C = O: 1.199(2) (**2**), 1.1917(17) (**3**), 1.091(3), 1.136 (3) (**mixture 2–3**) and 1.2010(16) (**5**). Color scheme: O: red, C: gray and H: grey.

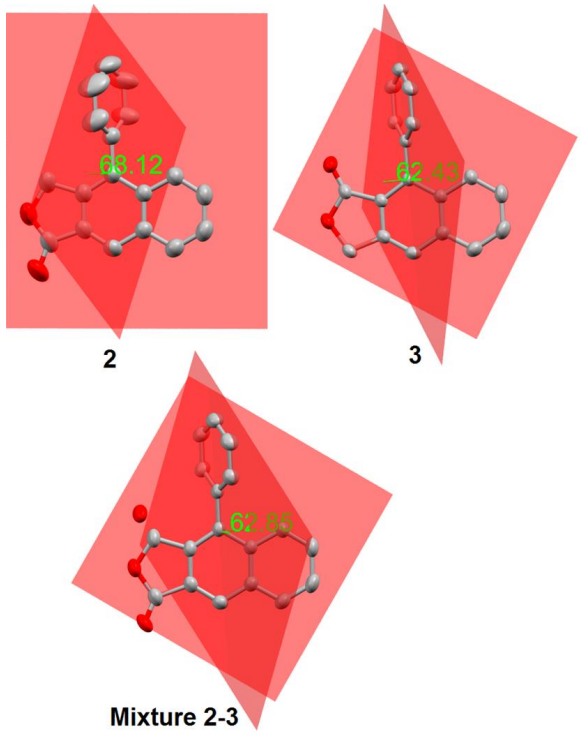

Figure 2. The torsion angles (°) between the phenyl group and the naphthofuranone moiety: **2**: 68.12°, **3**: 62.43° and **mixture 2–3**: 62.85°.

In structures **2** and **3** and **mixture 2–3** and **5**, intermolecular close-contacts were observed, forming a chain packing along the b-axis. Structures **2**, **3** and **mixture 2–3** all have a C2 rotation symmetry with intermolecular close-contact distances of 2.607 Å (**3**), 2.52 Å (**2**), 2.639 Å (**mixture 2–3**) and angles of 160.15° (**3**) 133.63° (**2**), 160.44° (**mixture 2–3**). However, structure **5** has mirror symmetry with an intermolecular close-contact distance of 2.629 Å and an angle of 146.79° (Figure 3).

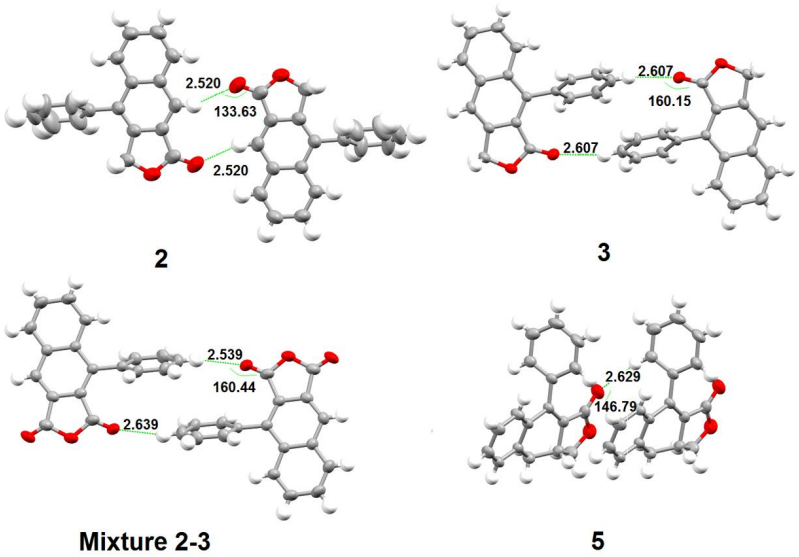

Figure 3. Intermolecular close-contacts in **2**, **3**, **mixture 2–3** and **5**.

Compound **5** has two sp^3 hydrogens on the lactone and can be fully aromatized to compound **3** when heated at higher temperatures in the presence of Pd/C. A similar structure was published by Amer et al. [26] with the only difference being the double-bond position in the cyclohexene ring [26]. A different symmetry of packing found in that case was also consistent with the published space group [26]. The structures of **2**, **3** and **mixture 2–3** have an isostructural unit cell (monoclinic $P2_1/c$), while the structure of **5** has a monoclinic $P2_1/n$ unit cell. Packing views along the a-axis are also shown in Figure 4 for all the structures. In the unit cell packing, four independent structures were placed in the asymmetric unit in a volume of approximately 1300 $Å^3$.

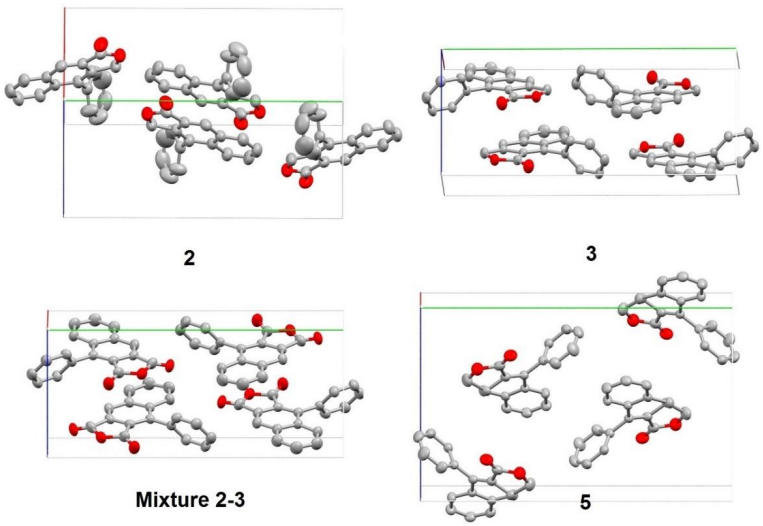

Figure 4. Packing of unit cell view along the a-axis in **2**, **3**, **mixture 2–3** and **5**. All H atoms are omitted for clarity.

4. Conclusions

The investigation of a Dehydro-Diels–Alder synthetic method for the synthesis of arylnapthalene lactones led to a set of high yield crystalline products. Four crystal structures of arylnapthalene lactones' bare scaffolds were collected and discussed in this communication. This method provided us with a set of fully characterized X-ray structures of arylnaphthalene lactones 2 and 3, a partially aromatic intermediate 5, as well as a unique mix-isomer structure (**mixture 2–3**). This mixture containing both arylnapthalene lactones isomers of Type I and Type II in the crystal is an interesting find and could further help with the bioactivity and therapeutic studies of these compounds. CCDC 2,092,032 (**2**), 2,092,033 (**3**), 2,092,034 (**mixture 2–3**) and 2,092,035 (**5**) contain the supplementary crystallographic data for this paper. These data can be obtained free of charge from The Cambridge Crystallographic Data Centre.

Supplementary Materials: The following are available online at https://www.mdpi.com/article/10.3390/cryst11080857/s1, $^{1}H/^{13}C$ NMR spectra of all compounds described **1–5** (Figures S1–S5), asymmetric unit for **mixture 2,3** (Figure S6) and packing diagrams of compounds **2**, **3 mixture 2,3** and compound **5** (Figures S7–S10).

Author Contributions: Conceptualization, N.M. and S.C.; methodology, N.M. and W.Z.; software, W.Z.; validation, W.Z.; formal analysis, W.Z.; investigation, N.M.; resources, N.M. and W.Z.; data curation, W.Z.; writing—original draft preparation, N.M., S.C. and W.Z.; writing—review and editing, N.M. and W.Z.; visualization, W.Z.; project administration, N.M. All authors have read and agreed to the published version of the manuscript.

Funding: The authors would like to thank the Simon Fraser University Dean of Science Office and the Chemistry Department for their generous financial support.

Institutional Review Board Statement: Not applicable.

Informed Consent Statement: Not applicable.

Data Availability Statement: Not applicable.

Acknowledgments: The authors would like to thank D. Leznoff (Simon Fraser University) for his critical review of this manuscript.

Conflicts of Interest: The authors declare no conflict of interest.

References

1. Calvo-Flores, F.G.; Dobado, J.A.; Isac-García, J.; Martín-MartíNez, F.J. (Eds.) *Biological Properties of Lignans. Lignin and Lignans as Renewable Raw Materials*; John Wiley & Sons: Hoboken, NJ, USA, 2015; pp. 369–454.
2. Vasilev, N.P.; Ionkova, I. Cytotoxic activity of extracts from Linum cell cultures. *Fitoterapia* **2005**, *76*, 50–53. [CrossRef] [PubMed]
3. Asano, J.; Chiba, K.; Tada, M.; Yoshii, T. Antiviral activity of lignans and their glycosides from Justicia procumbens. *Phytochemistry* **1996**, *42*, 713–717. [CrossRef]
4. Cow, C.; Leung, C.; Charlton, J.L. Antiviral activity of arylnaphthalene and aryldihydronaphthalene lignans. *Can. J. Chem.* **2000**, *78*, 553–561. [CrossRef]
5. Navarro, E.; Alonso, S.J.; Trujillo, J.; Jorge, E.; Pérez, C. Central nervous activity of elenoside. *Phytomedicine* **2004**, *11*, 498–503. [CrossRef] [PubMed]
6. Zhao, C.; Rakesh, K.P.; Mumtaz, S.; Moku, B.; Asiri, A.M.; Marwani, H.M.; Manukumar, H.M.; Qin, H.-L. Arylnaphthalene lactone analogues: Synthesis and development as excellent biological candidates for future drug discovery. *RSC Adv.* **2018**, *8*, 9487–9502. [CrossRef]
7. Stevenson, R.; Weber, J.V. Improved Methods of Synthesis of Lignan Arylnaphthalene Lactones via Arylpropargyl Arylpropiolate Esters. *J. Nat. Prod.* **1989**, *52*, 367–375. [CrossRef]
8. Li, J.-H.; Tang, J.-S.; Xie, Y.-X.; Wang, Z.-Q.; Deng, C.-L. Phosphazene Base-Catalyzed Intramolecular Cascade Reactions of Aryl-Substituted Enynes. *Synthesis* **2010**, *18*, 3204–3210. [CrossRef]
9. Foley, P.; Eghbali, N.; Anastas, P.T. Advances in the methodology of a multicomponent synthesis of arylnaphthalene lactones. *Green Chem.* **2010**, *12*, 888–892. [CrossRef]
10. Park, J.-E.; Lee, J.; Seo, S.-Y.; Shin, D. Regioselective route for arylnaphthalene lactones: Convenient synthesis of taiwanin C, justicidin E, and daurinol. *Tetrahedron Lett.* **2014**, *55*, 818–820. [CrossRef]
11. Kao, T.T.; Lin, C.C.; Shia, K.S. The Total Synthesis of Retrojusticidin B, Justicidin E, and Helioxanthin. *J. Org. Chem.* **2015**, *80*, 6708–6714. [CrossRef] [PubMed]

12. Eghbali, N.; Eddy, J.; Anastas, P.T. Silver-Catalyzed One-Pot Synthesis of Arylnaphthalene Lactones. *J. Org. Chem.* **2008**, *73*, 6932–6935. [CrossRef] [PubMed]
13. Park, S.; Kim, J.-H.; Kim, S.-H.; Shin, D. Transition Metal-Mediated Annulation Approaches for Synthesis of Arylnaphthalene Lignan Lactones. *Front. Chem.* **2020**, *8*, 628. [CrossRef] [PubMed]
14. Gudla, V.; Balamurugan, R. Synthesis of Arylnaphthalene Lignan Scaffold by Gold-Catalyzed Intramolecular Sequential Electrophilic Addition and Benzannulation. *J. Org. Chem.* **2011**, *76*, 9919–9933. [CrossRef] [PubMed]
15. Naresh, G.; Kant, R.; Narender, T. Silver(I)-Catalyzed Regioselective Construction of Highly Substituted α-Naphthols and Its Application toward Expeditious Synthesis of Lignan Natural Products. *Org. Lett.* **2015**, *17*, 3446–3449. [CrossRef] [PubMed]
16. Kocsis, L.S.; Brummond, K.M. Intramolecular dehydro-Diels-Alder reaction affords selective entry to arylnaphthalene or aryldihydronaphthalene lignans. *Org. Lett.* **2014**, *16*, 4158–4161. [CrossRef] [PubMed]
17. Rajesh, U.C.; Losovyj, Y.; Chen, C.-H.; Zaleski, J.M. Designing Synergistic Nanocatalysts for Multiple Substrate Activation: Interlattice Ag–Fe_3O_4 Hybrid Materials for CO_2-Inserted Lactones. *ACS Catal.* **2020**, *10*, 3349–3359. [CrossRef]
18. *SAINT*, Version 7.46A; Bruker Analytical X-ray System: Madison, WI, USA, 1997–2007.
19. *SADABS*, V2.10, Bruker Nonius Area Detector Scaling and Absorption Correction; Bruker AXS Inc.: Madison, WI, USA, 2003.
20. *TWINABS*, V2008/2, Bruker Nonius Scaling and Absorption for Twinned Crystals; Bruker AXS Inc.: Madison WI, USA, 2008.
21. *TWINABS*, V1.05, Bruker Nonius Scaling and Absorption for Twinned Crystals; Bruker AXS Inc.: Madison, WI, USA, 2007.
22. Altomare, A.; Burla, M.C.; Cammalli, G.; Cascarano, M.; Giacovazzo, C.; Guagliardi, A.; Moliterni, A.G.G.; Polidori, G.; Spagna, A. SIR97: A new tool for crystal structure determination and refinement. *J. Appl. Crystallogr.* **1999**, *32*, 115–119. [CrossRef]
23. Altomare, A.; Cascarano, G.; Giacovazzo, C.; Guagliardi, A.J. Completion and refinement of crystal structures with SIR92. *J. Appl. Crystallogr.* **1993**, *26*, 343–350. [CrossRef]
24. *SHELXTL*, Version 5.1; Bruker AXS Inc.: Madison, WI, USA, 1997.
25. Farrugia, L.J. ORTEP-3 for Windows—A version of ORTEP-III with a Graphical User Interface (GUI). *J. Appl. Crystallogr.* **1997**, *30*, 565. [CrossRef]
26. Amer, A.; Ho, D.; Rumpel, K.; Schenkel, R.I.; Zimmer, H. Substituted gamma-butyrolactones. Part 37: Reactions of (arylmethylene)furandiones with nucleophiles. A novel approach to the cyclolignan lactone skeleton. *J. Org. Chem.* **1991**, *56*, 5210–5213. [CrossRef]